Vol 14 No 5, May 2005
1009-1963/2005/14(05)/0953-06

Chinese Physics

© 2005 Chin. Phys. Soc.
and IOP Publishing Ltd

Spectra of highly ionized nickel*

Yang Zhi-Hu(杨治虎)[a)†], Du Shu-Bin(杜树斌)[b)], Zeng Xian-Tang(曾宪堂)[b)], Su Hong(苏 弘)[a)], Wang You-De(王友德)[a)], and Zhang Yan-Ping(张艳萍)[a)]

[a)] *Institute of Modern Physics, Chinese Academy of Sciences, Lanzhou* 730000, *China*

[b)] *Department of Nuclear Physics, China Institute of Atomic Energy, Beijing* 102413, *China*

(Received 15 December 2003; revised manuscript received 26 October 2004)

The spectrum of highly ionized nickel in the region 12–40nm was studied by means of the beam-foil method. Nickel ions of 45 and 70MeV were provided by the HI-13 tandem accelerator at China Institute of Atomic Energy. Numerous lines attributed to Ni XIII to XX transitions have been identified, and eighteen lines of them were newly measured.

Keywords: spectra, highly-ionized, beam-foil technique
PACC: 3220J, 3450H, 3220N

1. Introduction

Since nickel element is the second most abundant transition element in the sun after iron, the identification of the spectrum of nickel at high ionization stages is important for the study of the solar spectrum. The ions ranging from Ni XIII to Ni XX produce resonance transitions in the extreme ultraviolet spectral range starting from about 10nm. These ions are formed in the solar corona, and some of the resonance transitions have been observed in the solar spectra.[1] These transitions are also expected to be present in the spectra of many solar-type stars, as well as in those of other astrophysical objects.

In the present paper we give a classification of the emission spectra of Ni XIII to Ni XX in the wavelength region of 12–35nm. The transitions we discussed lie mainly between levels of principal quantum number n=2 to n=4; and the main data published for these transitions were obtained from laser-produced plasmas and theta-pinch plasmas. This work aims at giving a comprehensive account of the spectra of nickel at high ionization stages using the beam–foil method. In our present work, the spectral analysis is based on the comparison with previous experimental data and related theoretical results.

2. Experiment

A general description of the experimental set-up was given in Ref.[2], while some details of the light-collecting system is given here. The experiment was performed at the HI-13 tandem accelerator at the China Institute of Atomic Energy (CIAE). The heavy-ion accelerator, with a maximum terminal voltage of 15MV (but usually running at 2–14MV), is equipped with several kinds of ion sources. In this experiment, multiply charged Ni ions were accelerated to 45 and 70MeV, and directed through a 25μg/cm^2 carbon foil. The radiation emitted by the foil-excited ion was analysed with a 2.2 metre grazing incidence GIM-957 XUV–VUV monochromator, and equipped with a 600 lines/mm grating. The angle of incidence was 88.5°. The spectrometer viewed the beam at 90°, and its entrance slit was placed close to the ion beam with 6mm diameter, i.e. 7.5 mm from the centre of the beam. Using a 20μm entrance slit, the full width at half maximum of the spectral lines was about 0.04nm, yielding a wavelength uncertainty of less than 0.005nm for the majority of the identified lines. During the experiment, the beam currents ranging from 0.4 and 0.5μA were used, a microcomputer-controlled scan and the channetron detector were moved along the Rowland circle increment of the chordal distance of 0.1mm, and the light intensity at each point was normalized to a fixed amount of beam charge collected in a Faraday cup. In order to separate the electrons emitted by the

*Project supported by the National Natural Science Foundation of China (Grant Nos 10274088, 10275042 and 10134010).
†E-mail: z.yang@impcas.ac.cn

foil from the Faraday cup itself, a suppressor ring with a potential of 300 V was placed in front of the Faraday cup.

Wavelength calibration was made by using static sources of helium and argon, and the wavelengths were further corrected for Doppler shift by taking into account the 90° viewing angle. The accuracy of this angle was verified by means of the well-known 2s–2s2p line of S XIII 25.668nm. In this work, the discrepancies between the measured wavelengths and wavelengths taken as reference were always lower than 0.005nm.

3. Results and discussions

Since the accelerating process ensured a high degree of beam purity, and in the recorded spectra we never observed lines that might be ascribed to the excitation of the carbon of the foil, the observed lines were attributed solely to the incident ions. The identification of the lines in this work were very simple due to the previous excellent experimental results and the unique charge state calculation made possible by Nikolaev and Dimitriev[3] and Liu.[4] Additional support of the identification is given by observing the intensity variation of the lines as a function of beam energy. Figure 1 shows a partial spectrum in the experiment at 45 and 70MeV. A majority of the identified transitions are given in Tables 1–8 together with previous observations and theoretical wavelengths. Whenever possible our data are compared with previously published values, which enables us to test the accuracy of our measurements.

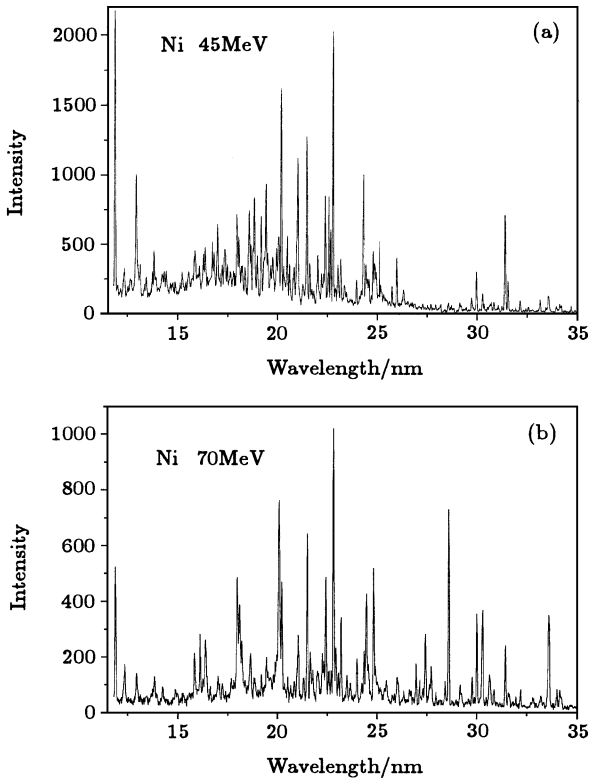


Fig.1. Beam-foil spectrum of nickel in 11.8–35nm.

3.1. F-like sequence

In addition to transitions involving high quantum numbers ($n \geq 4$) which may be predicted roughly neglecting the core polarization, numerous transitions belonging to $2p^4$ (^{3}P)3l and $2p^4$ (^{1}D)3l configurations have been identified for the F-like sequence. The classification was based on the comparison with previous beam–foil experimental data.[5] These results are given in Table 1.

Table 1. Spectra of F I-like nickel.

Transition	Wavelength/nm	
	This experiment	Other experiment[5]
5–6	18.625	18.616
6–7	18.746	18.740
$2p^43p^2F_{5/2}$–$2p^43d\ ^2G_{7/2}$	26.050	26.052
$2p^43p^4D_{7/2}$–$2p^43d\ ^4F_{9/2}$	27.555	27.555
7 – 9	28.232	28.236
$2p^43s^4P_{5/2}$-$2p^43p\ ^4D_{7/2}$	31.257	31.266
$2p^43s^2D_{5/2}$–$2p^43p\ ^2F_{7/2}$	32.590	32.597
$2p^43s^4P_{3/2}$–$2p^43p\ ^4D_{5/2}$	34.654	34.650

3.2. Ne-like sequence

Numerous transitions belonging to $2p^53d$ and $2p^53p$ configurations for Ne-like sequence have been identified. The wavelength determination was based on the variation of the wavenumber of the transitions with net charge ξ=N+1 along the isoelectronic sequence. Our wavelength measurements together with earlier observation of Buchet *et al*[6] and theoretical

results[7] are given in Table 2.

Table 2. Spectra of Ne I-like nickel.

Transition	Wavelength/nm		
	This experiment	Other experiment[5]	Theory[6,7]
$2p^5 3p\ ^1P_1$–$2p^5 3d\ ^1P^o_1$	16.426		16.40
$2p^5 3p\ ^3S_1$–$2p^5 3d\ ^3F^o_2$	16.914		16.92
$2p^5 3p\ ^2D_3$–$2p^5 3d\ ^3D^o_2$	18.217		18.25
$2p^5 3p\ ^3P_2$–$2p^5 3d\ ^3D^o_2$	19.174		19.17
$2p^5 3p\ ^3P_2$–$2p^5 3d\ ^3F^o_2$	19.405		19.44
$2p^5 3s\ ^3P^o_2$–$2p^5 3d\ ^3P_1$	20.900		20.96
$2p^5 3p\ ^3P_1$–$2p^5 3d\ ^1P^o_1$	21.394		21.39
$2p^5 3p\ ^3S_1$–$2p^5 3d\ ^3P^o_2$	22.552	22.534	22.55
$2p^5 3p\ ^3D_3$–$2p^5 3d\ ^3D^o_3$	23.492	23.490	23.43
$2p^5 3p\ ^3D_3$–$2p^5 3d\ ^1D^o_2$	24.047	24.040	24.05
$2p^5 3p\ ^1P_1$–$2p^5 3d\ ^1D^o_2$	24.563	24.565	24.566
$2p^5 3p\ ^1D_2$–$2p^5 3d\ ^1F^o_2$	25.043	25.039	25.06
$2p^5 3p\ ^1D_2$–$2p^5 3d\ ^3D^o_2$	25.487		25.48
$2p^5 3s\ ^2D_2$–$2p^5 3p\ ^2D_1$	29.786	29.790	29.802
$2p^5 3s\ ^3P^o_2$–$2p^5 3p\ ^1P_1$	29.856	29.842	29.87
$2p^5 3s\ ^3P^o_1$–$2p^5 3p\ ^1D_2$	30.382	30.380	30.37
$2p^5 3s\ ^3P^o_2$–$2p^5 3p\ ^3D_3$	30.624	30.630	30.63
$2p^5 3s\ ^1P^o_1$–$2p^5 3p\ ^1P_1$	31.490	31.501	31.49
$2p^5 3d\ ^3D^o_1$–$2s2p^6 3s\ ^3S_1$	32.820	32.824	32.82
$2p^5 3s\ ^1S_1$–$2p^5 3p\ ^1P_2$	34.808	34.805	34.817

3.3. Na-like sequence

Spectra of Na-like nickel are compared with the observations of Fawcett *et al*[8] and Buchet *et al*[5,6]. All the measured results and theoretical calculations[10−12] are given in Table 3.

Table 3. Spectra of Na I–like nickel.

Transition	Wavelength/nm		
	This experiment	Other experiments	Theory[10−12]
$4p^6 4f\ ^2F_{5/2}$ –$2p^6 5g\ ^2G_{7/2}$	12.401		
$2p^6 3p\ ^2P_{1/2}$–$2p^6 3d\ ^2D_{3/2}$	22.043	22.041[5], 22.043[8]	22.041
$2p^6 3p\ ^2P_{5/2}$–$2p^6 3d\ ^2D_{9/2}$	22.986	22.971[5]	22.932
$2p^6 3p\ ^2P_{3/2}$–$2p^6 3d\ ^2D_{5/2}$	23.377	23.376[5], 23.375[8]	23.379
$2p^6 3p\ ^2P_{3/2}$–$2p^6 3d\ ^2D_{3/2}$	23.627	23.635[5], 23.631[8]	23.636
$2p^6 4f\ ^2F_{7/2}$ –$2p^6 5g\ ^2G_{9/2}$	24.803	24.810[5]	
$2p^6 3s\ ^2S_{1/2}$–$2p^6 3p\ ^2P_{3/2}$	29.199	29.199[5], 29.201[8]	29.200
$2p^6 3s\ ^2S_{1/2}$–$2p^6 3p\ ^2P_{1/2}$	32.056	32.056[5], 32.056[8]	32.056

3.4. Mg-like sequence

Our results, together with the results of laser-produced spectra of nickel.[11] as well as theoretical results[12] are given in Table 4 for Mg-like sequence. In this work, the experimental measurements allow us to complete these data which may have a better spectroscopic quality, and to show a different excitation mechanism which can be seen from the comparison of line intensities. On the other hand, although some lines in our spectra are either blended or partially masked by others, their presence is doubtless because they appear in the neighbouring element. We have mentioned the indication of the blended lines in Table 4. In this case the uncertainty can be as high as 0.02nm.

Table 4. Spectra of Mg I-like nickel.

Transition	Wavelength/nm		
	This experiment	Other experiments	Theory[13]
$3p^2\ ^1D_2$ – $3p3d\ ^1F_3$	17.534	17.531[5], 17.540[12]	17.581
$3s3p\ ^3P_0$ –$3s3d\ ^3D_1$	19.735	19.725[5], 19.730[12]	19.739
$3s3p\ ^3P_1$ –$3s3d\ ^3D_2$	19.981	19.986[5], 19.987[12]	19.987
$3s3p\ ^3P_1$ –$3s3d\ ^3D_1$	20.055	20.052[5], 20.055[12]	20.053
$3p^2\ ^1D_2$ – $3p3d\ ^3D_3$	20.211	20.205[12]	
$3p^2\ ^3P_1$– $3p3d\ ^3D_2$	20.325		20.389
$3p^2\ ^3P_1$– $3p3d\ ^3D_1$	20.428		20.439
$3p^2\ ^3P_0$– $3p3d\ ^3P_1$	20.620		20.643
$3s3p\ ^3P_2$ –$3s3d\ ^3D_3$	20.755	20.748[5], 20.752[12]	20.750
$3p^2\ ^3P_1$– $3p3d\ ^3P_1$	21.172(+Ni XVI)	21.197[5], 21.171[12]	
$3s3p\ ^1P_1$ –$3s3d\ ^1D_2$	21.580	21.590[12]	
$3p^2\ ^1D_2$– $3p3d\ ^1D_2$	22.608	26.611[5], 22.609[12]	
$2s^2\ ^1S_0$– $3s3p\ ^1P_1$	24.920	24.922[5], 24.919[12]	24.918
$3s3p\ ^3P_1$ –$3p^2\ ^3P_2$	25.192	25.205[5], 25.195[12]	25.197
$3s3p\ ^3P_0$ –$3p^2\ ^3P_1$	26.358	26.358[12]	26.355
$3s3p\ ^3P_2$ –$3p^2\ ^3P_2$	26.606	26.606[12]	26.606
$3s3p\ ^3P_1$ –$3p^2\ ^3P_1$	26.936	26.942[12]	26.939
$3s3p\ ^3P_1$ –$3p^2\ ^1D_2$	27.304	27.309[12]	
$3s3d\ ^3D_2$ –$3p3d\ ^3D_3$	27.734(+Ni XX)	27.731[5]	27.771
$3s3d\ ^3D_3$ –$3p3d\ ^3D_3$	27.903	27.913[5], 27.916[12]	
$3s3p\ ^3P_1$ –$3p^2\ ^3P_0$	28.151	28.155[5], 28.147[12]	28.150
$3s3p\ ^3P_2$ –$3p^2\ ^3P_1$	28.305	28.312[12]	
$3s3p\ ^3P_2$ –$3p^2\ ^3P_1$	28.559	28.555[5]	28.559
$3s3d\ ^1D_2$–$3p3d\ ^1F_3$	29.031	29.025[5], 29.023[12]	
$3s3d\ ^3D_3$–$3p3d\ ^3F_4$	32.208	32.211[5], 32.203[12]	
$3s3d\ ^3D_2$–$3p3d\ ^3F_3$	33.8.28	22.819[5], 33.821[12]	

3.5. Al-like sequence

The analysis of nickel lines of Al-like sequence emitted by using the beam–foil technique has led to an extensive analysis of the nickel spectrum. The nickel lines were previously observed from a theta-plasma by Fawcett and Hayes,[14] some of the lines were found in the solar spectrum. In Table 5 we give some identifications based on the experimental results of Fawcett and Hayes[14] and the calculation of Fawcett.[13]

Table 5. Spectra of Al I-like nickel.

Transition	Wavelength/nm		
	This experiment	Other experiments	Theory[13]
$3s3p^2\ ^2D_{3/2}$ –$3s3p3d\ ^2F_{5/2}$	16.624		16.624
$3s3p^2\ ^2D_{5/2}$ –$3s3p3d\ ^2F_{5/2}$	16.785		16.741
$3s3p^2\ ^2D_{5/2}$ –$3s3p3d\ ^2F_{7/2}$	16.824		16.832
$3s3p^2\ ^2P_{1/2}$ –$3s3p3d\ ^2P_{1/2}$	19.329		19.330
$3s3p^2\ ^2D_{3/2}$ –$3s3p3d\ ^2D_{3/2}$	21.059		21.040
$3s^23p^2P_{1/2}$ –$3s3p^2\ ^2P_{3/2}$	21.856	21.830[5], 21.839[14]	21.850
$3s^23p^2P_{1/2}$ –$3s3p^2\ ^2P_{1/2}$	22.321	22.308[5], 22.309[14]	22.315
$3s^23p^2P_{3/2}$ –$3s3p^2\ ^2P_{3/2}$	23.255	23.249[5], 23.249[14]	23.248
$3s^23p^2P_{3/2}$ –$3s3p^2\ ^2P_{1/2}$	23.756	23.752[5], 23.787[14]	23.787
$3s^23p^2P_{1/2}$ –$3s3p^2\ ^2S_{1/2}$	23.955	23.937[5], 23.953[14]	23.955
$3s^23p^2P_{3/2}$ –$3s3p^2\ ^2D_{5/2}$	30.925	30.964[5], 30.940[14]	30.959
$3s^23p^2P_{3/2}$ –$3s3p^2\ ^2P_{3/2}$	31.366		31.367

3.6. Si–like sequence

Lines of Si-like nickel are given in Table 6. The identifications are based on the earlier observation of Fawcett *et al.*[14]

Table 6. Si I-like nickel.

Transition	Wavelength/nm	
	This experiment	Other experiment[14]
$3s^23p^2\ ^1D_2 - 3s^23p3d\ ^1F_3$	17.371	17.373
$3s^23p^2\ ^3P_0 - 3s^23p3d\ ^3P_1$	17.646	17.670
$3s^23p^2\ ^3P_2 - 3s^23p3d\ ^3D_3$	17.914	17.928
$3s^23p^2\ ^3P_2 - 3s^23p3d\ ^3D_1$	18.026	18.006
$3s^23p^2\ ^3P_2 - 3s^23p3d\ ^3P_2$	18.936	18.921
$3s^23p^2\ ^1D_2 - 3s^23p3d\ ^1D_2$	19.541	19.552
$3s^23p^2\ ^3P_2 - 3s3p^3\ ^3S_1$	22.191	22.193
$3s^23p^2\ ^1D_2 - 3s3p^3\ ^1P_1$	22.400	22.404
$3s^23p^2\ ^3P_2 - 3s3p^3\ ^1D_3$	31.907	31.901

3.7. P-like sequence

Table 7 gives the spectra of some lines of P-like nickel in this experiment and the observation of Fawcett and Hayes.[14]

Table 7. P I-like nickel.

Transition	Wavelength/nm	
	This experiment	Other experiment[14]
$3p^3\ ^2D^o_{3/2} - 3p^2(^1D)3d\ ^2D_{3/2}$	17.037	17.050
$3p^3\ ^4S^o_{3/2} - 3p^2(^3P)3d\ ^4P_{5/2}$	17.145	17.137
$3p^3\ ^2D^o_{5/2} - 3p^2(^3D)3d\ ^2D_{5/2}$	17.221	17.216
$3p^3\ ^2P^o_{1/2} - 3p^2(^1D)3d\ ^2P_{1/2}$	17.779	17.756
$3s^23p^3\ ^4S^o_{3/2} - 3s3p^4\ ^2P^o_{5/2}$	31.645	31.653

3.8. S–like sequence

Three lines of S-like nickel are given in Table 8. Wavelength identification is based on the experimental results of Fawcett.[13]

Table 8. S I-like nickel.

Transition	Wavelength/nm	
	This experiment	Other experiment[14]
$3p^4\ ^3P_2 - 3p^3(^4S)3d\ ^3D_3$	15.771	15.773
$3p^4\ ^3P_1 - 3p^3(^4S)3d\ ^3D_2$	15.994	15.997
$3p^4\ ^3P_1 - 3p^3(^2D)3d\ ^3P_2$	16.396	16.415

From the above tables we can see that our experimental results show good agreement with the theoretical predictions in all cases, and other available experimental results. There are eighteen lines in Tables 2–8, which have not been found in the previously published experimental work for the classification of Ni XIII–Ni XX spectra between 12nm and 35nm, and show reasonable agreement with theory. These lines are identified as $2p^53p\ ^1P_1$–$2p^53d\ ^1P^o_1$, $2p^53p\ ^3S_1$–$2p^53d\ ^3F^o_2$, $2p^53p\ ^2D_3$–$2p^53d\ ^3D^o_2$, $2p^53p\ ^3P_2$–$2p^53d\ ^3D^o_2$, $2p^53p\ ^3P_2$–$2p^53d\ ^3F^o_2$, $2p^53s\ ^3P^o_2$–$2p^53d\ ^3P_1$, $2p^53p\ ^3P_1$–$2p^53d\ ^1P^o_1$ and $2p^53p\ ^1D_2$–$2p^53d\ ^3D^o_2$ transitions of Ne–like sequence at 16.426; 16.914; 18.217; 19.174; 19.405; 20.900; 21.394 and 25.487nm; $4p^64f\ ^2F_{5/2}$ –$2p^65g\ ^2G_{7/2}$ transition of Na – like nickel at 12.401nm; $3p^2\ ^3P_1$– $3p3d\ ^3D_2$, $3p^2\ ^3P_1$– $3p3d\ ^3D_1$ and $3p^2\ ^3P_0$– $3p3d\ ^3P_1$transitions of Mg-like sequence at 20.325; 20.428 and 20.620nn; $3s3p^2\ ^2D_{3/2}$ –$3s3p3d$

$^2F_{5/2}$, $3s3p^2\ ^2D_{5/2}$ –$3s3p3d\ ^2F_{5/2}$, $3s3p^2\ ^2D_{5/2}$ – $3s3p3d\ ^2F_{7/2}$, $3s3p^2\ ^2P_{1/2}$ –$3s3p3d\ ^2P_{1/2}$, $3s3p^2\ ^2D_{3/2}$ –$3s3p3d\ ^2D_{3/2}$ and $3s^23p^2P_{3/2}$ –$3s3p^2\ ^2P_{3/2}$ transitions of Al–like sequence at 16.624, 16.785, 16.824, 19.329, 21.059 and 31.366nm. These lines are regarded as new lines.

Acknowledgements

We wish to thank the staff of the HI-13 tandem accelerator at the China Institute of Atomic Energy (CIAE) for providing the ion beam.

References

[1] Behring W E, Cohen L and Feldman U 1972 *Astrophys. J.* **175** 493
[2] Zeng X T 1999 *Spectroscopic Studies of Highly Ionized Atoms* (Sweden: Lund University Press)
[3] Nikolev V S and Dimitriev I S 1968 *Phys. Lett.* **28** A 277
[4] Liu Z J 2000 *Chin. Phys.* **49** 687
[5] Buchet-Poulizac M C and Buchet J P 1988 *Nucl. Instrum. Methods* B **31** 182
[6] Buchet J P, Buchet-Poulizac M C, Denis A and Desesquelles J 1987 *J. Phys.* B **20** 1709
[7] Hibbert A, Le Dourneuf M and Mohan M 1993 *At. Data Nucl. Data Tables* **53** 23
[8] Fawcett B C, Cowan R D and Hayes R W 1972 *J. Phys.* B **5** 2143
[9] Kim Y K and Cheng K T 1978 *J. Opt. Soc. Am.* **63** 836
[10] Tull C E, McEachran R P and Cohen M 1971 *At. Data* **3** 167
[11] Froese Fischer C 1976 *Phys. Scr.* **14** 269
[12] Churilov S S, Kononov E Ya, Ryabtsev A N and Zayikin Yu F 1985 *Phys. Scr.* **32** 501
[13] Fawcett B C 1983 *At. Data Nucl. Data Tables* **28** 579
[14] Fawcett B C and Hayes R W 1972 *J. Phys.* B **5** 366